Mathematical Modeling and Algorithm Application
ISSN: 3006-0842 | Vol. 6, No. 2, 2025

Development of a Dual/Multi-Beam Interferometric Epitaxial Layer Thickness Calculation Model Integrating FFT and Least Squares Method

Lei Sun[1, *], Dongrui Lai[2], Chenyue Zhang[1], Xianwang Zhang[1]

[1]School of Mechatronic Engineering, Xi'an Technological University, Xi'an, China
[2]Electronic Information Engineering, Xi'an Technological University, Xi'an, China
[*] **Corresponding author**: Lei Sun (Email: 2825256897@qq.com)

Abstract: This paper proposes methods related to epitaxial layer thickness detection and inversion calculation, focusing on the exploration of epitaxial layer thickness calculation models based on the interference principle and the application of corresponding algorithms. Firstly, a specific dispersion model is adopted to fit the refractive index of the epitaxial layer, and an appropriate error metric is used to evaluate the fitting degree. Combined with Snell's law and Fresnel equations, the reflection and transmission coefficients are calculated. The optical path difference and total phase difference under variable refractive index are derived through integration, thereby establishing a thickness measurement model. Secondly, the Fast Fourier Transform (FFT) is utilized to obtain the initial thickness value. Combined with a weighted joint least squares optimization model, a specific algorithm combination is employed to invert the thickness. A resampling method is used to determine the confidence interval, ensuring a good fitting effect. Finally, the necessary conditions for multi-beam interference and the reflectivity formula are derived, and a multi-beam thickness calculation model is established. This model has a better goodness of fit and can correct the deviations of the previous model. Integrating multiple algorithms, the proposed model balances accuracy and efficiency, exhibits excellent fitting performance and strong robustness, and can accurately realize the detection of epitaxial layer thickness.

Keywords: Fast Fourier Transform, Least Squares Method, Double-Beam Interference.

1. Introduction

This paper focuses on the optical detection and inversion calculation of epitaxial layer thickness, aiming to establish an accurate thickness measurement system based on interference principles and adaptive algorithms to address the core technical challenges in detecting epitaxial layer thickness under variable refractive index conditions [1]. First, leveraging the mid-infrared spectral characteristics, the LST dispersion model is selected to fit the epitaxial layer refractive index, with the fitting accuracy validated by root mean square error. Refractive angles and related parameters are then derived from Snell's law. The Fresnel equations calculate reflection and transmission coefficients for different polarization components. Integration determines optical path differences and total phase differences under variable refractive indices, establishing a fundamental dual-beam interferometric thickness measurement model. Second, addressing the nonlinear relationship between thickness, wavenumber, and reflectance, the initial thickness range was first locked using Fast Fourier Transform (FFT) on the interference oscillation frequency to avoid local optima [2]. A joint least-squares objective function incorporating signal-to-noise ratio weighting and multi-class constraints was then constructed. Variable projection and a derivative-free one-dimensional search algorithm were iteratively applied to refine the precise thickness, with residual resampling analyzing result reliability. Finally, the method is extended to multi-beam interference scenarios. The necessary conditions for interference and reflectivity formulas are derived to establish a multi-beam thickness model, correcting the systematic bias of the dual-beam model [3]. Experimental results demonstrate that the constructed model exhibits high fitting accuracy and robustness, enabling precise detection of epitaxial layer thickness and providing a reliable technical solution for relevant fields.

2. Epitaxial layer thickness detection via double-beam interference

2.1. Fitting of epitaxial layer refractive index

According to the common segmentation in spectroscopy, the data are mainly concentrated in the mid-infrared region, and the reflectivity extreme region does not change with the incident angle. Among the commonly used dispersion models, a fitting method is selected, and it is found that the LST model [4] can well meet this condition. The fitting process is carried out as follows:

$$n(v)=\sqrt{\frac{\sqrt{\varepsilon_1(v)^2+\varepsilon_2(v)^2}+\varepsilon_1(v)}{2}} \tag{1}$$

The Root Mean Square Error (RMSE) is used as the error metric to evaluate the fitting degree. The fitting curves and measured curves of reflectivity at incident angles of 10° and 15° are obtained, as shown in the Figure 1:

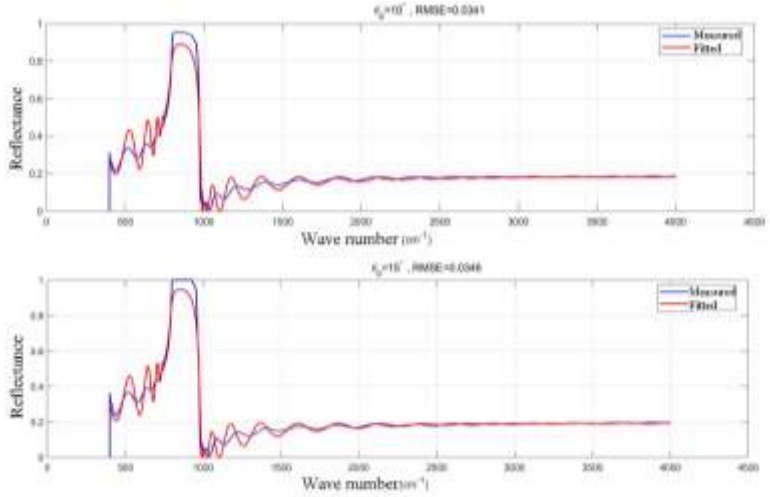


Figure 1. Fitted and measured curves of reflectivity at incident angles of 10° and 15°

The Root Mean Square Error (RMSE) values, which serve as the error metrics for evaluating the fitting degree, are 0.0341 and 0.0346 at incident angles of 10° and 15°, respectively. Both values are less than 0.1, indicating an excellent prediction accuracy.

2.2. Determination of reflectivity

Let the incident angle be θ_i and the refraction angle be θ_r. After clarifying the geometric optical path through analysis, it is found that this interference is similar to thin-film interference, and thus the geometric solution approach for thin-film interference can be considered for application.

According to Snell's law, at the interface from the air layer to the epitaxial layer, the refraction angle and the cosine value corresponding to the refraction angle can be calculated once the incident angle is known, as follows:

$$n_0 \sin\theta_i = n(\lambda)\sin\theta_r(\lambda) \tag{2}$$

$$r_{s1} = \frac{n_0\cos\theta_i - n(\lambda)\cos\theta_r(\lambda)}{n_0\cos\theta_i + n(\lambda)\cos\theta_r(\lambda)}, \qquad t_{sl} = \frac{2n_o\cos\theta_i}{n_o\cos\theta_i + n\cos\theta_r} \tag{4}$$

The same logic applies to the p component.

A refraction occurs at the interface from the epitaxial layer to the air. According to the law of conservation of energy:

$$t_{s1}t'_{s1} = 1 - r_{s1}^2 \tag{5}$$

The values of t'_{s1} and t'_{p1} are derived respectively as follows:

$$t'_{s1} = \frac{1-r_{s1}^2}{t_{s1}}, \qquad t'_{p1} = \frac{1-r_{p1}^2}{t_{p1}} \tag{6}$$

where n_0 denotes the refractive index of air. Further derivation yields:

$$\sin\theta_r(\lambda) = \frac{\sin\theta_i}{n(\lambda)}, \qquad \cos\theta_r(\lambda) = \sqrt{1-\frac{\sin^2\theta_i}{n^2(\lambda)}} \tag{3}$$

The same principle applies to the interface from the epitaxial layer to the substrate.

The reflection coefficients and transmission coefficients can be calculated using the Fresnel equations. Since the reflection coefficient of reflected ray 1 is required, and the refracted ray corresponds to the reflected ray at the substrate interface, it is necessary to determine the reflection coefficients and transmission coefficients for the s and p components at the interface from the air layer to the epitaxial layer.

The reflection coefficient r_{s1} and transmission coefficient t_{s1} for the s component are given by:

where t'_{s1} and t'_{p1} represent the s-component and p-component of the transmission coefficient at the interface from the epitaxial layer to the air, respectively.

Based on the interference intensity formula, the total reflected light intensity $I_{Rs}(\lambda)$ for the s component and $I_{Rp}(\lambda)$ for the p component are obtained separately:

$$\begin{aligned} I_{Rs}(\lambda) &= I_{r1s}(\lambda) + I_{r2s}(\lambda) + 2\sqrt{I_{r1s}(\lambda)I_{r2s}(\lambda)}\cos\Delta\varphi_s(\lambda), \\ I_{Rp}(\lambda) &= I_{r1p}(\lambda) + I_{r2p}(\lambda) + 2\sqrt{I_{r1p}(\lambda)I_{r2p}(\lambda)}\cos\Delta\varphi_p(\lambda) \end{aligned} \tag{7}$$

Further, the total reflectivity $R_s(\lambda)$ for the s component and $R_p(\lambda)$ for the p component are derived:

$$R_s(\lambda)=\frac{I_{Rs}(\lambda)}{I_0},\quad R_p(\lambda)=\frac{I_{Rp}(\lambda)}{I_0} \tag{8}$$

In laboratory settings, the infrared light employed in the infrared interference method is typically unpolarized. Therefore, the total reflectivity is expressed as:

$$R(\lambda)=\frac{R_s(\lambda)+R_p(\lambda)}{2} \tag{9}$$

2.3. Determination of phase difference

The phase difference mainly consists of two components: the optical path difference caused by light propagation in the epitaxial layer and the potential phase jump resulting from interface reflection.

(1) As light propagates back and forth in the epitaxial layer, and the refractive index of the epitaxial layer is not a constant [5], each change in the refractive index leads to a change in refraction within the epitaxial layer. To solve the trajectory of this optical path in the silicon carbide epitaxial layer, calculus is applied to this process. The phase difference $\Delta\varphi_1(\lambda)$ caused by the optical path difference is obtained as follows:

$$\Delta\varphi_1(\lambda)=\frac{2\pi}{\lambda}2\int_0^d n(\lambda)\frac{dx}{\cos\theta_r(\lambda)} \tag{10}$$

where x represents the position along the thickness direction of the epitaxial layer, with a range of $0\le x\le d$.

(2) If $r_{s1}(\lambda)<0$, the s-component of reflected light 1 undergoes a phase jump of π; if $r_{s2}(\lambda)<0$, the s-component of reflected light 2 exhibits an additional phase jump of π. The same principle applies to the p-component. By adding the phase differences $\Delta\varphi_{2s}(\lambda)$ and $\Delta\varphi_{2p}(\lambda)$ caused by reflection phase jumps to the phase difference caused by the optical path difference, the total phase difference is obtained:

$$\Delta\varphi_s(\lambda)=\Delta\varphi_1(\lambda)+\Delta\varphi_{2s}(\lambda),\quad \Delta\varphi_p(\lambda)=\Delta\varphi_1(\lambda)+\Delta\varphi_{2p}(\lambda) \tag{11}$$

2.4. Establishment of the layer thickness measurement model

Based on the above analysis, the following equation is derived:

$$\begin{aligned}R(\lambda)=\frac{1}{2}\Big(&|r_{s1}(\lambda)|^2+|t_{s1}(\lambda)|^2|r_{s2}(\lambda)|^2|t'_{s1}(\lambda)|^2+2|r_{s1}(\lambda)||t_{s1}(\lambda)||r_{s2}(\lambda)||t'_{s1}(\lambda)|\cos\left(\Delta\varphi_s(\lambda)\right)\\&+|r_{p1}(\lambda)|^2+|t_{p1}(\lambda)|^2|r_{p2}(\lambda)|^2|t'_{p1}(\lambda)|^2+2|r_{p1}(\lambda)||t_{p1}(\lambda)||r_{p1}(\lambda)||t'_{p1}(\lambda)|\cos\left(\Delta\varphi_p(\lambda)\right)\Big)\end{aligned} \tag{12}$$

where both $\Delta\varphi_p(\lambda)$ and $\Delta\varphi_s(\lambda)$ are related to the thickness of the epitaxial layer.

3. Inversion calculation of epitaxial layer thickness

To obtain the epitaxial layer thickness value, the Fast Fourier Transform (FFT) is first used to quickly estimate an initial thickness value that is relatively close to the true value from the frequency of interference oscillations. Subsequently, the least squares fitting method is employed, utilizing all data points across the entire spectrum for iteration to obtain an accurate solution.

3.1. Optimization model for epitaxial layer thickness

3.1.1. Objective Function

For the spectral data $\{R_{10^\circ,\text{meas}}(\nu),R_{15^\circ,\text{meas}}(\nu)\}$ corresponding to the two sets of incident angles (10° and 15°), a joint least squares objective function is constructed as follows:

$$\min \mathrm{L}(d)=\sum_{\tilde{\nu}}\left[w_{10^\circ}(\nu)\cdot\left(R_{10^\circ,\,\text{model}}-R_{10^\circ,\,meas}\right)^2+w_{15^\circ}(\nu)\cdot\left(R_{15^\circ,\,\text{model}}-R_{15^\circ,\,meas}\right)^2\right] \tag{13}$$

where $R_{\theta,\text{model}}$ denotes the theoretically calculated reflectivity at an incident angle of θ, and the weight $w_\theta(\nu)$ is set based on the local signal-to-noise ratio (SNR)—wavelength intervals with higher SNR are assigned larger weights. By minimizing this objective function, the epitaxial layer thickness d that minimizes the discrepancy between the theoretical reflectivity and the measured reflectivity at both incident angles can be determined.

3.1.2. Constraint Conditions

Physical Constraints: The solution must be physically meaningful. The epitaxial layer thickness must be a positive value, and the weights in the least squares model must also be positive, i.e.,

$$d>0\ ,\quad w_\theta(\nu)>0 \tag{14}$$

Constraint on the Refractive Index Distribution Function:

If the refractive index $n(\nu)$ across the entire layer is always greater than $n_0 \sin\theta$, the bottom interface is accessible, i.e.,

$$n_0 \sin\theta < n(\nu) \tag{15}$$

Constraint on the Absolute Value of the Amplitude Coefficient: If the absolute value $|A| is too small, the interference fringes become indistinct, and such data points are unsuitable for thickness fitting, i.e.,

$$|A| > \text{ò} \tag{16}$$

Boundary Constraint on Reflectivity: Theoretically, the energy reflectivity satisfies

$$R_{\theta,\text{model}} \in [0,1] \tag{17}$$

In summary, the optimization model for the optimal epitaxial layer thickness is established.

3.2. Algorithm design

The model has used FFT to lock the target to the local optimal region, enabling the least squares method to quickly and accurately find the global optimal solution within this local range. There is no need to select global algorithms or multi-dimensional algorithms requiring gradients; instead, the variable projection method—which has extremely high computational efficiency for handling linear parameters—is adopted, combined with a one-dimensional search method that does not require derivative calculation and has a fast convergence rate to optimize d.

3.2.1. FFT Initial Screening for Initial Value

The Fast Fourier Transform (FFT) is an efficient algorithm for computing the Discrete Fourier Transform (DFT). The purpose of DFT is to convert a signal from the time domain or spatial domain to the frequency domain. First, a resampling variable $x = \nu(n(\nu)/\cos\theta_r(\nu))$ is introduced to correct the influence of refractive index dispersion, making the phase difference $\Delta\phi(x) = 4\pi dx$ a linear function of x. Second, the interference signal in the x-domain can be approximated as a single-frequency oscillation; the main frequency f_x obtained by performing FFT on it satisfies $f_x = 2d$ (where d is in centimeters). After this transformation, the frequency of interference fringes is proportional to the film thickness. Using FFT processing can effectively avoid the problem of local convergence. The algorithm steps are as follows:

Step 1) Data preprocessing: Calculate some pre-quantities first to facilitate subsequent model processing.

Step 2) Construct the pure interference oscillation signal and convert it to the linear domain: $\hat{y}(x) = \dfrac{R_{\text{meas}}(x) - B(x)}{A_{\text{ref}}(x)}$; discard data points where $|A| < \text{ò}$—at these points, the fringes are almost invisible, and elimination is necessary to avoid polluting the frequency spectrum.

Step 3) Apply a window function to $\hat{y}(x)$, then perform FFT, and extract the main peak frequency f_x from the frequency spectrum.

Step 4) Derive the initial thickness value based on the frequency-thickness relationship:

$$d_{0,\text{cm}} = \frac{f_x}{2}, \quad d_{0,\mu\text{m}} = 5\times10^3 \cdot f_x \tag{18}$$

Step 5) Calculate the ratio of the main peak height to the side lobe height. If the signal-to-noise ratio is higher than the threshold, the FFT initial value is considered reliable; otherwise, the grid search method is used to re-estimate the initial value.

The solution results are as follows: The initial value of $\text{FFT}10^\circ\text{d}$ is 7.36813722 μm, the initial value of $\text{FFT}15^\circ\text{d}$ is 6.952860553 μm, the combined initial value reaches 7.160498887 μm, and the final thickness estimate is 6.802473942 μm.

3.3. Solution results and reliability analysis

3.3.1. Establishment of Confidence Interval

To obtain a more robust result, it is necessary to calculate the 95% confidence interval for the thickness d. The formula is expressed as follows:

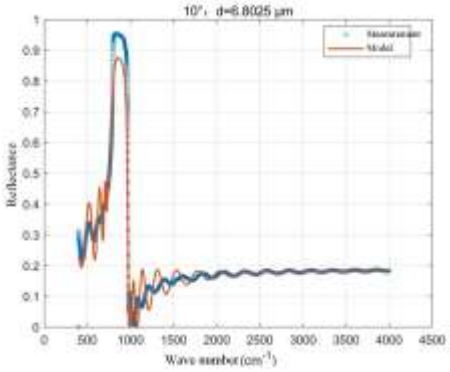
$$d \pm 1.96\sqrt{\text{Cov}_{dd}} \tag{19}$$

where Cov_{dd} denotes the diagonal element corresponding to the thickness d in the covariance matrix, representing the variance of the thickness d.

The Bootstrap method is used for resampling the residuals with replacement. Multiple sets of reflectivity data are generated to calculate residuals, and the distribution of these thickness estimates is statistically analyzed. The 2.5th and 97.5th percentiles of the distribution are computed, thereby determining the 95% confidence interval for the epitaxial layer thickness d: the upper bound is 6.79749015 μm, and the lower bound is 6.807457734 μm.

3.3.2. Algorithm Solution Results

The optimized thickness d is substituted into the model to calculate the theoretical reflectivities $R_{10^\circ,\text{model}}$ and $R_{15^\circ,\text{model}}$. The graphs representing the measured values and fitted values of reflectivity at incident angles of 10° and 15° are shown in Figure 2:



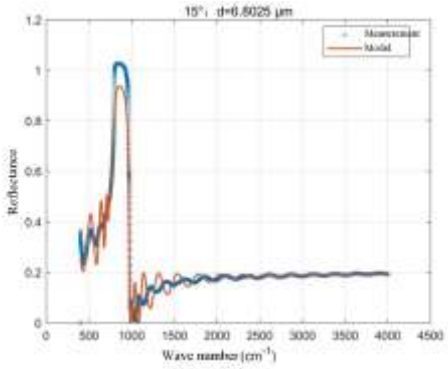


Figure 2. Fitted Curves of Double-Beam Interference at Incident Angles of 10° and 15°

The calculated goodness-of-fit (coefficient of determination, R^2 is 0.950 for an incident angle of 10° and 0.951 for an incident angle of 15°. Additionally, by observing the degree of overlap between the measured curves and the fitted curves, it is evident that the two pairs of curves (corresponding to 10° and 15° incident angles) overlap highly. This indicates an excellent fitting effect of the model.

4. Model multi-beam interference model and epitaxial layer thickness calculation

Light waves undergo multiple reflections and transmissions at the epitaxial layer interface and the substrate interface, forming multi-beam interference. The analysis starts from the scenario where only one reflection at each of the two interfaces is considered, and then extends to the case of multiple reflections and transmissions.

4.1. Deduction of necessary conditions for multi-beam interference

Multiple reflections and transmissions within the epitaxial layer led to the accumulation of optical path differences, and additional phase jumps may also occur. The magnitude of interface reflectivity affects the intensity of reflected light, which can result in the failure to form clear interference fringes [6]. Since the incident light is derived from the same beam, only the constancy of the phase difference between two coherent beams after multiple reflections needs to be considered. The interference condition for any two reflected beams (m, n) is:

$$\Delta\varphi_{m,n} = \varphi_m - \varphi_n = 2k\pi, \quad k \in \mathbb{Z} \tag{20}$$

As long as two beams satisfy the above condition, interference between them will occur.

When $R(\lambda)$ (reflectivity) is very small, the intensity of the reflected light decreases rapidly after reflection, making the interference unobservable. However, excessively high reflectivity leads to extremely narrow passbands, which also hinders observation.

In summary, multi-beam interference affects the final accuracy of the thickness d through two aspects: the cumulative effect on the phase difference and its own sensitivity to the interface reflectivity.

4.2. Epitaxial layer thickness calculation model under multi-beam interference

Multi-beam interference can be regarded as the superposition of all reflected lights, where the interference term of two beams is transformed into the interference sum of an infinite number of beams. The solution of the multi-beam interference reflectivity formula is considered using the form of complex amplitude, with the influences on the s-component and p-component analyzed separately.

For the s-component, the complex amplitude of the m-th reflected light is:

$$E_{s,m} = r_{s1}t_{s1}t_{s1}r_{s2}^{m-1}e^{-i(m-1)\Delta\varphi_s} \cdot E_{s,0} \tag{21}$$

where $E_{s,0}$ is the complex amplitude of the s-component of the incident light, and $m = 1, 2, \ldots, m = 1$ corresponds to the reflection at the air→epitaxial layer interface, and $m \geq 2$ corresponds to multiple round-trip reflections. The complex amplitude of the s-component of the total reflected light is the sum of an infinite series. Using the sum formula of the infinite geometric series, the reflectivity of the s-component is obtained, and through complex number operations and algebraic simplification, the following result is derived:

$$R_s = \frac{|r_{s1}|^2\left(1-|r_{s1}|^2\right)^2}{1+|r_{s2}|^2-2|r_{s2}|\cos\left(\Delta\varphi_s\right)} \tag{22}$$

The R_p of the p-component is similar. Then, the total reflectivity of multi-beam interference is:

$$R = \frac{1}{2}(R_s + R_p) \tag{23}$$

By continuing to use the established model, the thickness detection model under the condition of multi-beam interference can be derived. The thickness d obtained from the algorithm solution is 3.5195 μm, and the residuals of the two curves at incident angles of 10° and 15° are 0.12811 and 0.14136, respectively. The visualization is shown as in the Figure 3.

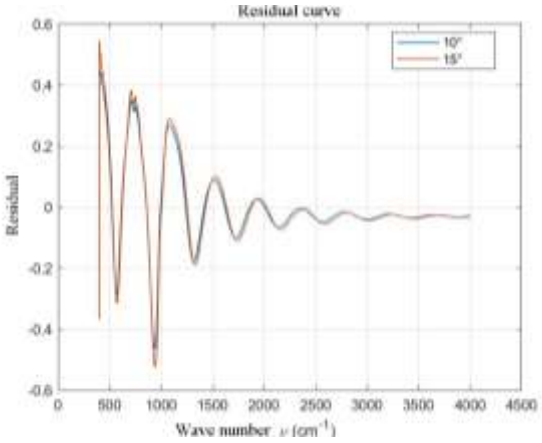


Figure 3. Residual Variation Curves Under the Multi-Beam Interference Model

As can be seen from the figure, the global fitting accuracy is relatively high, with residuals fluctuating within the range

of ± 0.6 ; the variation trends of the two curves (corresponding to incident angles of 10° and 15° are highly consistent, indicating that the established model has good robustness.

4.3. Correction of layer thickness calculation by the multi-beam interference model

If the fitting effect of the multi-beam interference model is better than that of the double-beam model under the same conditions, it can be determined that the silicon carbide test data are interfered by the multi-beam interference effect. In this case, the multi-beam interference model can be directly used to correct the epitaxial layer thickness.

Under the multi-beam interference model, the goodness-of-fit R^2 values obtained for incident angles of 10° and 15° are 0.9828 and 0.9847, respectively. Both values are close to 1, indicating an excellent fitting effect and high model accuracy.

Residual Plot. Compared with the results obtained from the double-beam interference model, the residual of the multi-beam interference model is smaller. The corrected value of the epitaxial layer thickness under the multi-beam interference condition is calculated as: $d = 7.1190\,\mu\mathrm{m}$.

5. Conclusions

This paper proposes a dual-beam interferometry system for epitaxial layer thickness detection, incorporating thickness inversion calculations and a multi-beam interferometric correction model. This approach efficiently addresses thickness measurement challenges under variable refractive indices, delivering both high precision and robust performance. First, the dual-beam model employs the LST dispersion model to fit refractive indices (RMSE < 0.1). It combines Snell's law and the Fresnel equations to calculate polarization component parameters, integrates to determine optical path differences and phase differences, and achieves a reflectance fitting goodness-of-fit R^2 exceeding 0.95, closely matching experimental data. Second, the inversion model employs FFT to lock the initial thickness to avoid local optima. It utilizes a constrained joint least squares function with variable projection iteration, combined with Bootstrap sampling to determine the 95% confidence interval. The final inverted thickness is approximately 6.80, yielding reliable results. Subsequently, the multi-beam model derived interference conditions and reflectivity formulas, correcting dual-beam deviations to elevate R^2 above 0.98 with reduced residual fluctuations. Finally, the model achieved full-process coverage from measurement to inversion and correction, adapting to diverse interference scenarios. Future research may further optimize adaptability to multi-material epitaxial layers.

References

[1] Han Xu. Analysis of Doping Concentration for Silicon Carbide Epitaxial Wafers Used in Automotive 1200V SiC MOSFETs [J]. China Science and Technology Information, 2025(15):135-137.

[2] Ye Fuqiu. FFT-Based Fourier Spectrum Analysis Using MATLAB Simulation[J]. Journal of Jishou University (Natural Science Edition), 2011, 32(01): 49-51+62.

[3] Hu Yong, Pan Dongming, Wu Rushang, et al. Least-Squares Inverse Time Shift with Combined Amplitude-Phase Estimation in Time-Frequency Domain [J]. Chinese Journal of Geophysics, 2021, 64(01): 209-223.

[4] Lv Yonglin, Zheng Wanxiang, Li Rujie, et al. Measurement of Optical Constants and Thickness of Thin Films Based on Reflectance Spectroscopy [J]. Infrared Technology, 2024, 46(08): 965-973.

[5] Zhou Qibiao, Chen Jianhua, Song Yuhua, et al. Design and Analysis of Variable Refractive Index Optical Thin Films [J]. New Technology and New Process, 2020(05):47-51.

[6] Yao Qijun. Optical Tutorial [Textbook]. 4th ed. Beijing: Higher Education Press, 2008.